IIETA International Information and Engineering Technology Association
Advancing the World of Information and Engineering

Revue des Composites et des Matériaux Avancés-Journal of Composite and Advanced Materials
Vol. 35, No. 6, December, 2025, pp. 1129-1140
Journal homepage: http://iieta.org/journals/rcma

Effect of External Heat Source on Surface Roughness in Turning of Al/SiC Metal Matrix Composites: A Comparative Study of Optimization Methods

Veera Venkata Siva Sudheer Nakka[1*], Karteeka Pavan Kanadam[2], Ramgopal Reddy Bijjam[1], Srinivas Chandanam[1]

[1] Department of Mechanical Engineering, R.V.R. & J.C. College of Engineering, Chowdavaram, Guntur 522019, India
[2] Department of Computer Applications, R.V.R. & J.C. College of Engineering, Chowdavaram, Guntur 522019, India

Corresponding Author Email: nvvssudheer1969@gmail.com

https://doi.org/10.18280/rcma.350613

Received: 15 October 2025
Revised: 28 November 2025
Accepted: 19 December 2025
Available online: 31 December 2025

Keywords:
external heat source, carburizing flame, oxidizing flame, Al/Sic-MMC, BUE, surface roughness, MRR, Differential Evolution, WOA, Cuckoo Search, TLBO

ABSTRACT

This research experimentally examines the impact of external heat sources, specifically carburizing and oxidizing heat sources, on the surface quality obtained during the turning of Al/SiC metal matrix composites (Al/SiC-MMCs) on a lathe. A 3-level, 3-factor full factorial design was applied by considering cutting velocity, cutting feed, and cutting depth as variables. According to the experimental findings, empirical power-law analytical models were established to evaluate surface roughness. To optimize the cutting variables, the derived models and associated constraints were subjected to four metaheuristic optimization algorithms such as Differential Evolution (DE), Whale Optimization Algorithm (WOA), Cuckoo Search (CS), and Teaching Learning Based Optimization (TLBO). This study aims to find the most effective combination of cutting velocity, cutting feed, and cutting depth that would improve surface quality and enhance the Material Removal Rate (MRR). Experimental outcomes demonstrate that carburizing flame-assisted turning substantially improves surface quality (overall surface roughness decreased by 17.25%) compared to dry machining and turning assisted by an oxidizing flame. Among the optimization techniques, TLBO achieved the best optimization performance, consistently producing the least surface roughness value of 3.403, with cutting speed converging to 94 m/min, feed rate to 0.113 mm/rev, and depth of cut between 0.34 mm and 0.75 mm. Statistical analysis further confirmed TLBO's superiority, yielding the lowest mean fitness value (3.403), lowest standard deviation (0.005), and highest stability (95% of runs within ±0.005 of the best value). TLBO proved to be the most reliable and effective method for improving surface finish in machining.

1. INTRODUCTION

Al/SiC-based Metal Matrix Composites are extensively utilized in the manufacturing industries due to their excellent mechanical performance, thermal performance, and low weight per unit volume. These characteristics make Al/SiC MMCs suitable for applications in the automobile, aviation, and military sectors. However, the existence of hard ceramic filler particles, typically silicon carbide (SiC), makes machining these materials highly challenging. Taya and Arsenault [1] reported that the hardness of reinforcing particles in Al-MMCs often exceeds that of advanced cutting tools, resulting in accelerated tool wear and process instability. Manna and Bhattacharya [2] observed that during turning operations, the hard SiC particles dull the tool cutting edge, leading to a poor surface finish. In a subsequent study, Manna and Bhattacharya [3] noted that the combined effects of elevated temperature, pressure, and friction during machining can lead the softer aluminum matrix to stick to the cutting tool, creating a Built-Up Edge (BUE). This phenomenon further deteriorates surface integrity and complicates the machining process.

To mitigate these issues, Diniz and Micaroni [4] introduced the deployment of cutting fluids helps lower the temperature and cutting forces in the machining region by providing effective lubrication and cooling, which in turn reduces the friction at the cutting interface. However, conventional cutting fluids pose environmental and health hazards, and current global environmental regulations increasingly demand the reduction or elimination of such pollutants in industrial processes. Alternative approaches to improve machinability without resorting to cutting fluids have gained attention. Tash et al. [5] demonstrated that heat treatment processes can enhance the hardness of Al-MMCs and reduce BUE formation. Roy et al. [6] emphasized the need for special machining strategies to suppress BUE formation at both low and high cutting speeds, particularly to avoid chip adhesion and surface degradation. According to Sun et al. [7], the application of external thermal energy can transform brittle materials into ductile ones by lowering their yield strength, thereby improving machinability. Attia et al. [8] conducted comparative experiments between laser-assisted machining

(LAM) and conventional turning, concluding that LAM enhanced surface finish by over 25% and increased material removal rate (MRR) by up to 800%. Further innovation in this domain includes the hybrid technique of ultrasonic vibration-assisted hot turning, for beta-Ti alloy machining applications [9]. Their study reported significantly reduced cutting forces and enhanced surface finish relative to conventional turning. Their research showed a notable decrease in forces acting on the cutting zone and better surface finish relative to traditional turning. Yongho et al. [10] observed that incorporating energy from an external source while turning hard-to-machine materials significantly improves machining performance. Nevertheless, they highlighted that this field remains in its early stages, and a deeper understanding of underlying mechanisms and optimization strategies is required for broader industrial applications.

During the turning of aluminium-based materials such as Al/SiC, the inherent softness of the matrix results in the generation of continuous chips, which increases friction and promotes BUE formation at the tool tip, ultimately deteriorating the surface finish. The primary objective of this work is to mitigate these issues by modifying the surface characteristics through controlled heating (flame-assisted turning) and cooling during machining, thereby improving machinability and surface quality.

To accomplish the above objective, the experiments are performed to investigate the influence of the Carburizing heat source (which promotes continuous spin-hardening) and oxygen-rich oxy-acetylene flame as external heat sources on surface quality while turning of Al-based metal matrix composites. Results from these heat-assisted processes are compared with conventional dry machining.

A 3-level, 3-factor full factorial design (3^3) was employed, with cutting velocity, cutting feed rate, and cutting depth set at three distinct levels. Power-law regression models were formulated for each condition using multiple regression analysis. These models were further optimized using four metaheuristic algorithms-Differential Evolution, Whale Optimization Algorithm, Cuckoo Search, and Teaching Learning Based Optimization to identify the best processing parameters for optimizing surface roughness and material removal rate.

2. OPTIMIZATION ALGORITHM: A REVIEW

To identify the best machining parameters that enhance surface finish and the material removal rate, several advanced metaheuristic algorithms were employed in this study. These include Differential Evolution, Whale Optimization Algorithm, Cuckoo Search, and Teaching-Learning-Based Optimization. The following section outlines the characteristics, mechanisms, and applications of these algorithms.

The Differential Evolution algorithm, suggested by Price and Storn [11], is a stochastic, population-based evolution algorithm widely recognized for its simplicity, robustness, and strong performance in continuous, nonlinear, and multimodal optimization problems. DE operates by generating trial vectors through the scaled variation between randomly chosen individuals from the population, which are then combined with a target vector. If the trial vector yields an improved objective value, it substitutes the target vector within the population. The Differential Evolution algorithm is controlled by three main variables: mutation factor (F), rate of crossover (CR), and size of population (NP), which govern its exploration and exploitation capabilities. Swagatam et al. [12] highlighted DE's ease of implementation when compared with other evolutionary algorithms. Further research [13] verified that DE outperforms others in convergence rate, robustness, and solution accuracy. The algorithm has been successfully applied in engineering design, neural network training, and image processing. More recently, Wang and Yu [14] proposed an improved DE variant that integrates three distinct mutation strategies, enhancing convergence rate, solution accuracy, and population diversity across benchmark optimization functions.

The Whale Optimization Algorithm, developed by Seyedali and Andrew [15], is based on the bubble-net hunting behavior of humpback whales. It models three primary actions: surrounding the prey, performing bubble-net attacks (spiral updating), and searching for prey. These strategies help maintain a balance between local exploitation and global exploration of the solution space. WOA's simplicity, limited control parameters, and strong global search capabilities have contributed to its popularity across a broad spectrum of uses, particularly in engineering optimization, medical imaging, and signal processing. However, as noted by researchers, WOA may exhibit slow convergence in complex, high-dimensional search landscapes. A comprehensive review by Rana et al. [16], analyzing 82 studies, recommended hybridizing WOA with other techniques to enhance its convergence behavior and applicability.

The Cuckoo Search algorithm [17] is inspired by the brood parasitic strategy of cuckoos and incorporates Lévy flight patterns, along with the use of Lévy flights for random exploration. The algorithm replaces poor-performing nests (solutions) with new, potentially better ones, emulating the natural selection mechanism. CS is recognized for its rapid convergence, strong global search capability, and ease of implementation, making it applicable to numerous real-world challenges. It has been successfully utilized in engineering design applications. It has been applied effectively in engineering design, machine learning, and image processing domains. Gandomi et al. [18] validated the algorithm's performance across multiple optimization benchmarks. Additionally, Mostafa and Maral [19] used CS to optimize a novel float system design for experimental setups, demonstrating its practical utility. However, like many metaheuristics, the effectiveness of the algorithm is sensitive to parameter tuning.

The Teaching Learning Based Optimization algorithm, introduced by Rao et al. [20], mimics the teaching and learning dynamics in a classroom. This algorithm simulates the teaching and learning dynamics of a classroom, where learners (candidate solutions) improve their performance through interactions with the teacher (best solution) and peer learners. TLBO runs in two main phases: the teacher phase, which drives the average performance of the population closer to the teacher's level, and the learner phase, where mutual learning among students enhances knowledge diversity. TLBO is parameter-free, requiring only the population size and the total number of generations, which simplifies implementation. Due to its strong convergence behavior, minimal parameter dependency, and computational efficiency, the TLBO algorithm originally proposed by Rao [21] has found broad applications in domains such as mechanical design optimization, power system planning, and machine learning.

Palanikumar et al. [22] demonstrated that TLBO can

effectively improve cutting performance while reducing material wastage. Improved variants such as IMTLBO-RKSM, proposed by Ang et al. [23], have also reported better accuracy and diversity in Pareto solutions compared to conventional methods. Wang et al. [24] reported that the ERDE algorithm achieved nearly a 42% reduction in prediction error in surface-roughness estimation. In the domain of Cuckoo Search optimization, Qiang et al. [25] successfully applied CS-based methods to predict wear rate, output power, and surface roughness, demonstrating close agreement with experimental results. Enhanced CS variants such as the Coevolutionary Host-Parasite model, developed by Kalita et al. [26], further showed robust performance with minimal deviation in predicted optimal settings. Similarly, Kawecka [27] demonstrated that the Whale Optimization Algorithm (WOA) can effectively identify optimal parameters in abrasive waterjet machining, achieving results comparable to experimental benchmarks. Overall, these studies confirm that metaheuristic algorithms such as TLBO, DE, CS, and WOA offer strong potential for machining parameter optimization due to their accuracy, robustness, and consistency.

3. MATERIALS AND TOOLING DETAILS

A workpiece of Al/SiC metal matrix composite (Al-MMC) with a diameter of 75 mm procured from Pushp Trading Company Pvt Ltd, Hyderabad, was utilized for the experiments. The composite is reinforced with 15% silicon carbide (SiC) particles, 25 µm in Al6061 alloy and was specifically chosen due to its wide application in the automobile and aviation industries. The material has a Brinell hardness of 95BHN and a density of 2.7 g/cm^3. The tool holder of PSDNN 2525 M12 with a tool insert of SNMG120408-TN2000 grade (CVD coated carbide) with a back rake angle of -6º, side rake angle of -6º, and relief angle of -6º.

4. EXPERIMENTATION

A cylindrical Al/SiC metal matrix composite specimen of 75 mm diameter was employed for the experimental investigation. The machining tests were performed on a TMX/2030 engine lathe, capable of a greatest spindle speed of 1200 rpm. The main process variables—cutting velocities (v) of 34 m/min, 64 m/min, 94 m/min, cutting feeds(f) of 0.113 mm/rev, 0.178 mm/rev, 0.249 mm/rev, and cutting depths (d) of 0.25 mm, 0.5 mm, and 0.75 mm. The speed of cutting (34–94 m/min), cutting feed (0.113–0.248 mm/rev), and cutting depth (0.25–0.75 mm) selected for the 3^3 factorial design were chosen to ensure both practical relevance and safe machining conditions. These parameter ranges were defined following recommendations reported by Manna et al. [28] for turning Al/SiC-MMCs, as well as the operational limits of the lathe machine used in the experimental work. A total of 27 unique parameter combinations were tested under three different machining conditions: dry cutting, carburizing flame-assisted cutting (higher acetelene flow rate as compared to oxygen, such as 2.5:1 is used), and oxidizing flame-assisted cutting (higher oxygen flow rate as compared to acetelene, such as 2.5:1 is used).

Each condition was replicated twice, resulting in a total of 162 experiments [(3×3×3)×2×3]. For each trial, machining was performed over a length 10–15 mm. Al/SiCMMC bars measuring a length of 300 mm and a diameter of 75 mm were used, with 10 to 12 tests performed on each bar. Surface roughness was evaluated using a Surftest 211 profilometer (Mitutoyo, Japan) at three equally spaced points around the circumference, each separated by 120°, and the average of these measurements was used for further analysis (Figure 1).

Figure 1. Work piece and Surf test 211

Figure 2. Flame heating

4.1 Implementation of oxidizing heat source and carburizing heat source

In the process of turning, carburizing heat was applied to the workpiece, keeping a 4 cm distance between the torch tip and the workpiece surface, and maintaining an approximate 5 cm length of arc between the heat source and the tool interface. Post-heat treatment, the workpiece was immediately quenched using a water spray to achieve rapid cooling prior to the cutting process. This experimental setup is illustrated in Figure 2. An identical procedure was followed for the oxidizing flame heating (oxygen-rich flame), wherein the flame composition was adjusted accordingly to create an oxygen-rich environment.

4.2 Comparison of surface roughness under different machining conditions

Based on the results of the experimentals, the average surface roughness (Ra) parameters were determined for every machining parameter – cutting velocity (v), cutting feed (f),

and cutting depth (d) – across three machining environments: carburizing flame, oxidizing flame, and dry. The corresponding trend graphs between surface roughness and each cutting parameter were generated for comparative analysis and are shown in the Figures 3-5.

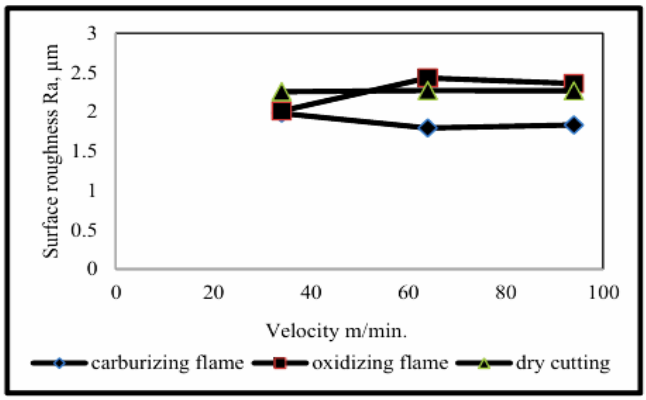

Figure 3. Cutting speed vs. surface roughness under different machining conditions

As illustrated in Figure 3, the surface roughness (Ra) exhibited distinct trends across the three cutting environments with respect to variations in cutting speed. Under the carburizing flame condition, surface roughness values were consistently lower compared to the dry and oxidizing flame conditions, demonstrating improved surface quality. The variation in Ra with increasing cutting speed in this condition was minimal, indicating a stable machining response.

In dry cutting, the surface roughness also exhibited limited variation with cutting speed, though the Ra values remained higher than those observed under carburizing flame. In contrast, under the oxidizing flame condition, surface roughness initially increased with cutting speed until a certain limit, after which it started to decrease, suggesting a non-linear response likely influenced by thermal and material interaction effects at elevated speeds. Overall, the dry cutting condition resulted in intermediate Ra values, falling between those of the carburizing and oxidizing flame environments. The variations in surface roughness expressed as percentages under carburizing and oxidizing conditions relative to dry cutting, across various cutting speeds. Key observations include:

- At a cutting velocity of 34 m/min, the surface roughness decreased by 12.16% under carburizing heat source and by 10.82% in the oxidizing flame condition, relative to the dry cutting conditions.
- While a cutting velocity of 64 m/min, the carburizing heat source led to a 21.02% decrease in surface roughness, while the oxidizing flame condition showed a 7.09% increase, relative to dry machining.
- When the cutting velocity was 94 m/min, the carburizing flame condition continued to show improvement, with a 15.42% reduction in Ra, whereas the oxidizing flame condition caused surface roughness to increase by 8.96% compared to the dry condition.

These findings indicate that carburizing flame-assisted turning can significantly enhance surface finish, especially at moderate cutting speeds, while oxidizing flame conditions may adversely affect surface quality at higher speeds.

As shown in Figure 4, surface roughness (Ra) increases in response to higher cutting feed across all three cutting environments. Of the three conditions, the carburizing flame-assisted machining consistently produced the lowest Ra values across all feed rates, followed by dry cutting, with oxidizing flame-assisted machining resulting in the highest roughness values.

- Under the minimum cutting feed of 0.113 mm/rev, carburizing flame heating caused a 25% decrease in Ra relative to the dry machining.
- When the cutting feed was raised to 0.178 mm/rev, the reduction in Ra for carburizing over dry cutting was approximately 18%.
- At the maximum cutting feed of 0.249 mm/rev, the carburizing flame condition showed a 15% improvement over dry cutting.

These results confirm that feed rate is a dominant factor influencing surface roughness, and that carburizing flame heating effectively mitigates roughness escalation, especially at lower feed rates.

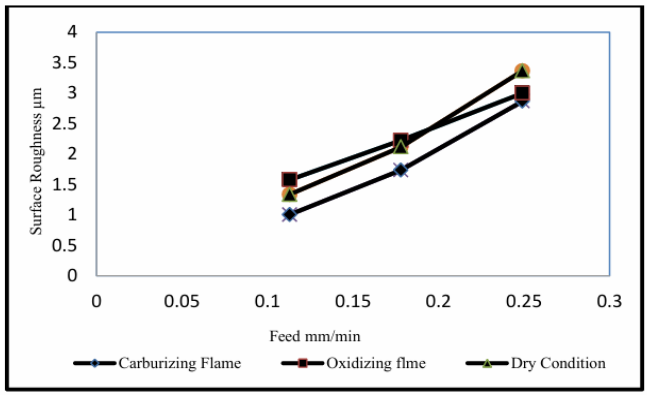

Figure 4. Feed rate vs. surface roughness under different machining conditions

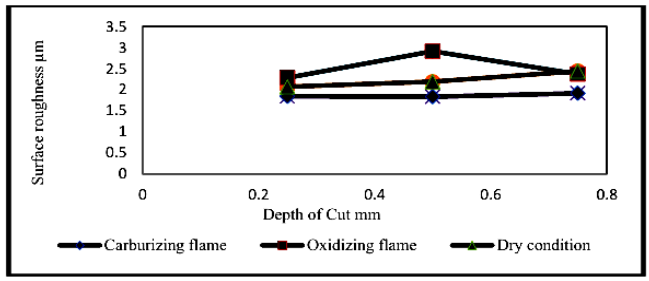

Figure 5. Effect of cutting depth on surface roughness under various cutting conditions

As presented in Figure 5, surface roughness (Ra) varies when changes in the cutting depth are exhibited consistently across all machining environments. Under the carburizing flame condition**,** surface roughness values remained the lowest across all depths of cut**,** and the variation in Ra was minimal, indicating a stable cutting condition and improved thermal management at the tool-material interface. During dry machining conditions, surface roughness showed only limited variation when cutting depth increased, with Ra values lying between those of carburizing and oxidizing flame conditions. The oxidizing flame condition, however, presented a non-linear trend: surface roughness increased up to a certain depth (0.50 mm), reached a peak, and then decreased at a higher depth (0.75 mm). This could be attributed to material softening effects or unstable thermal conditions at intermediate cutting depths.

The percentage changes in surface roughness for both flame-assisted conditions relative to dry cutting:

- When a cutting depth of 0.25 mm, Ra decreased by 10.91% under the carburizing flame condition compared to dry machining and by 10.48% in the oxidizing flame condition, relative to dry cutting.
- At 0.50 mm, the carburizing flame condition resulted in a 16.20% reduction, whereas the oxidizing flame condition showed a 33.10% increase in Ra.
- At 0.75 mm, the carburizing flame condition continued to provide surface quality improvement, with a 21.50% reduction in Ra relative to dry machining. Conversely, under the oxidizing flame condition, resulted in only a 2.82% decrease, suggesting diminishing returns at higher depths.

These results further confirm that carburizing flame-assisted turning is effective in minimizing surface roughness across varying depths of cut, while the oxidizing flame condition demonstrates inconsistent behavior, particularly at intermediate depths.

The improvement can be attributed to the localized surface hardening effect generated by the carburizing flame, which modifies the near-surface layer of the material prior to material removal. This thermal-chemical interaction increases the surface hardness of the Al matrix, thereby reducing the propensity of soft aluminium to cling to the cutting tool.

The increased hardness promotes discontinuous chip formation rather than continuous ductile chips, which effectively reduces cutting forces and friction at the interface between the tool and the chip. As a result, the likelihood of BUE formation is a common issue while machining aluminium alloys because of their high ductility and tendency to react with tool materials is significantly minimized. The suppression of BUE formation leads to more stable cutting action, lower tool workpiece interface temperature, and reduced tool wear, collectively resulting in improved surface integrity and better dimensional accuracy.

Therefore, carburizing flame assistance provides a beneficial machining environment for Al/SiC MMC by stabilizing chip formation, reducing adhesion-related wear mechanisms, and enhancing finished surface quality.

4.3 Analysis of Variance (ANOVA)

ANOVA was carried out to assess the influence of machining variables on surface roughness. under different cutting conditions.

Dry Cutting: The model was found to be statistically significant with an F-value of 16.06 and a p-value < 0.0001, indicating a strong collective contribution of the factors. Among the model terms, feed rate (f) showed the highest significance, with an F-value of 141.09 ($p < 0.0001$). All other factors, including speed of cutting (v), cutting depth (d), quadratic terms (v^2, f^2, d^2), and interaction effects (v×f, v×d, f×d), were statistically insignificant ($p > 0.05$). The model achieved a coefficient of determination of $R^2 = 0.8948$, demonstrating a strong correlation between predicted and experimental values.

The Pareto chart (Figure 6) of factor effects further confirmed that the model was significant, and feed rate was the most influential factor, whereas all remaining terms presented negligible influence on output response.

Carburizing Flame-Assisted Cutting: The ANOVA indicated a highly significant model with an F-value of 40.89 ($p < 0.0001$). Feed rate (f), its quadratic term (f^2), and the interaction term v × f were the most significant factors, with F-values of 352.47, 5.45, and 487, respectively. The remaining parameters, including v, d, quadratic effects (v^2, d^2), and interactions (v × d, f × d), were statistically insignificant ($p > 0.05$). The model demonstrated excellent predictive capability with $R^2 = 0.9325$.

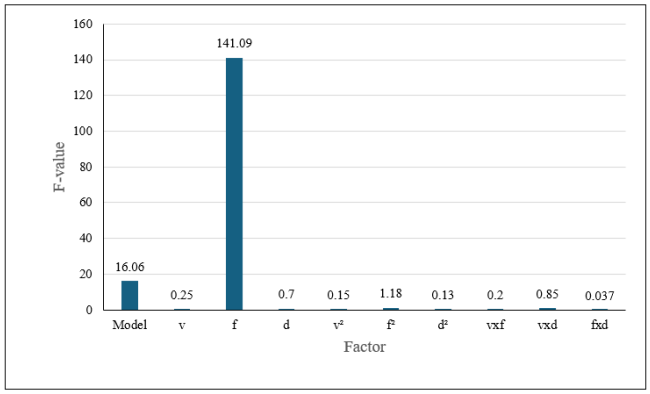

Figure 6. Pareto chart of ANOVA factor effects of dry cutting

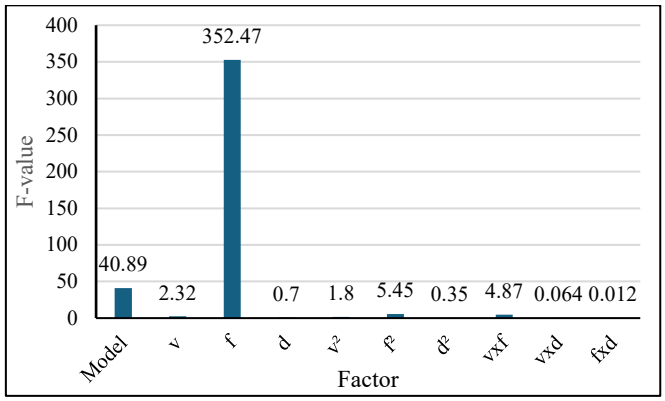

Figure 7. Pareto chart of ANOVA factor effects of carburizing flame assisted turning

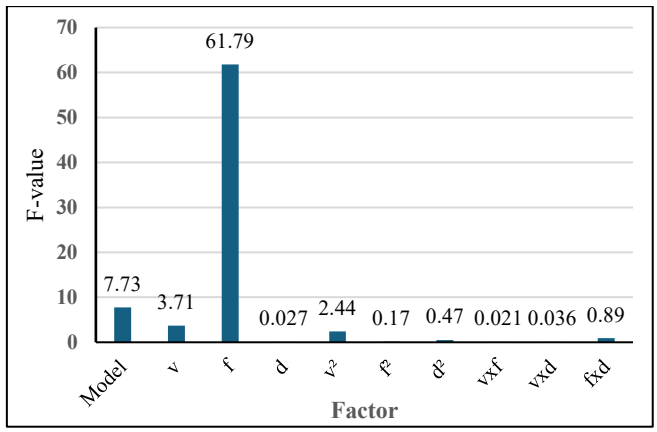

Figure 8. Pareto chart of ANOVA factor effects of oxidizing flame assisted turning

The Pareto chart of factor effects (Figure 7) further confirms the overall significance of the model, indicating that cutting feed has the strongest effect, with f^2 and v × f identified as the next significant contributors. The remaining factors show negligible influence on the output response.

Oxidizing Flame-Assisted Cutting: The model was also significant for oxidizing flame-assisted cutting, with an F-value of 7.73 ($p < 0.0002$), indicating a strong collective contribution of the factors. Feed rate (f) again exhibited the highest significance ($F = 61.79$, $p < 0.0001$), while all other terms, including v, d, quadratic, and interaction effects were insignificant ($p > 0.05$). The model achieved $R^2 = 0.8036$, indicating a strong correlation between predicted and experimental values.

The Pareto chart of factor effects (Figure 8) further validated the significance of the model, demonstrating that feed rate exerted the strongest influence, while the other factors contributed only marginally to the output response.

5. MATHEMATICAL MODEL FOR SURFACE ROUGHNESS

From the experimental findings, empirical power-law models were developed to predict surface roughness (Ra) for each machining environment-dry machining, carburizing heat source, and oxidizing heat source. The general equation of the model is shown in Eq. (1):

$$R_a = k\, v^a f^b d^c \tag{1}$$

In the above equation, v is the cutting velocity in m/min, f represents cutting feed (mm/rev), d represents the cutting depth in mm, and *k, a*, *b*, *c* are constants of the regression model determined from experimental data.

5.1 Surface roughness model for carburizing flame turning

Using the experimental results from carburizing flame-assisted turning, Surface roughness (Ra) was estimated using a power-law model of cutting parameters. The model is expressed as shown in Eq. (2):

$$R_a = 22.1005\, v^{-0.052} f^{1.32} d^{0.06} \tag{2}$$

where, the exponent of the cutting feed ($f^{1.32}$) is substantially larger than that of cutting velocity ($v^{-0.052}$) and cutting depth ($d^{0.06}$), indicating that cutting feed has the greatest influential factor in determining surface roughness under carburizing flame conditions.

This model can be reliably employed to estimate surface roughness for specified cutting parameters in carburizing flame-assisted turning of Al/SiC-MMCs.

5.2 Surface roughness model for oxidizing flame turning

The power-law model for surface roughness (Ra), derived from the experimental data from oxidizing flame turning, is given by Eq. (3):

$$R_a = 81.45\, v^{-0.356} f^{2.1} d^{0.106} \tag{3}$$

In this model, the exponent of cutting feed is significantly higher than that of cutting velocity and cutting depth, indicating that feed rate is the major factor influencing surface roughness in oxidizing flame-assisted turning.

This model can be efficiently utilized to forecast surface roughness under specified cutting conditions in oxidized flame-assisted turning of Al/SiC-MMCs.

5.3 Surface roughness model for dry cutting

According to the experimental findings from dry cutting, the surface roughness (Ra) is modelled using a power-law Eq. (4):

$$R_a = 22.83\, v^{-0.028} f^{1.28} d^{0.06} \tag{4}$$

As observed, the exponent of cutting feed is greater than that of cutting velocity and cutting depth, confirming that cutting feed is the major factor influencing surface roughness in dry cutting as well.

This model provides an effective means of predicting surface roughness for given machining conditions in dry turning of Al/SiC-MMCs.

6. COMPARISON OF OPTIMIZATION METHODS FOR OPTIMAL PROCESS PARAMETERS (v,f,d)

This study compares four optimization techniques, such as Differential Evolution, Whale Optimization Algorithm, Cuckoo Search, and Teaching Learning Based Optimization.

Each technique is used to optimize cutting velocity (v), cutting feed (f), and cutting depth (d) with the goals of minimizing surface roughness and maximizing MRR. This work experimentally investigates the impact of carburizing and oxidizing flames on surface finish during the turning of Al/SiC metal matrix composites. A 3^3 full factorial design was employed for the experiments. According to the data collected, analytical equations were formulated to represent the relationship among machining variables and outcomes. The optimization of these models was performed using Differential Evolution, Whale Optimization Algorithm, Cuckoo Search, and Teaching–Learning-Based Optimization to identify the best combination of cutting velocity, cutting feed, and cutting depth to achieve minimum surface roughness and maximum MRR. The results indicate that turning with a carburizing flame produces a superior surface quality relative to an oxidizing heat source and dry machining conditions. The optimization techniques were applied to determine global optimum values for the objective functions. The optimized parameters giving the least surface roughness were determined for turning using oxidizing, carburizing heat sources, and dry machining, with the goal of reducing surface roughness. The empirical models developed for each condition are expressed as follows:

$$SR1 = 22.1005\, v^{-0.052} f^{1.32} d^{0.06}$$

$$SR2 = 81.45\, v^{-0.356} f^{1.2} d^{0.106}$$

$$SR3 = 22.83\, v^{-0.028} f^{1.28} d^{0.06}$$

Maximization of:

$$\text{Material Removal Rate} = vfd \tag{5}$$

Subjected to constraints:

$$34 \le v \le 94$$
$$0.113 \le f \le 0.249$$
$$0.25 \le d \le 0.75$$

The problem is formulated as a multi-objective optimization given by Eq. (6), with the design criterion being the

minimization of:

$$Z = SR1 + SR2 + SR3 + \frac{1}{MRR} \quad (6)$$

Each algorithm was executed 100 times, using a population size of 20 and 30 iterations maximum.

Optimal process parameters of the model is determined using Differential Evolution, Whale Optimization Algorithm, Cuckoo Search, and Teaching-Learning-Based Optimization techniques to determine the best combination of cutting velocity, cutting feed, and cutting depth for reducing surface roughness and enhancing MRR. The detailed procedures for these methods are presented in this section.

6.1 Differential Evolution (DE) Procedure

DE is an evolutionary search method that evolves a population of candidate vectors by combining differences between members to create trial candidates; selection keeps only improvements by Das et al. [13].

Algorithm 1: Differential Evolution (DE)

Input: Population size N, scaling factor F, crossover rate CR, objective function f(x)
Output: Best candidate solution
Procedure:
Step 1: Initialize population of N candidates within bounds.

$$Z_i{}^t = \left[Z_{i.1}{}^t, Z_{i,2}{}^t, \ldots, Z_{i,d}{}^t\right]$$

Step 2: For each individual, generate a mutant vector using weighted differences of randomly selected vectors.

$$U_k{}^t = Z_m{}^t + F \times \left(Z_i{}^t - Z_j{}^t\right)$$

Step 3: Perform a crossover between the mutant and the target to form a trial vector.

$$U_{k,n}{}^{t+1} = \begin{matrix} U_{k,n}{}^t \ if \ r \le CR \\ Z_{k,n}{}^t \ otherwise \end{matrix}$$

Step 4: Evaluate fitness of trial; replace target if improved

$$Z_k{}^{t+1} = \begin{matrix} U_k{}^{t+1}, & if \ f\left(U_k{}^{t+1}\right) > f\left(Z_k{}^t\right) \\ Z_k{}^t, & if \ f\left(U_k{}^{t+1}\right) < f\left(Z_k{}^t\right) \end{matrix}$$

Step 5: Repeat until the termination criterion is met.

6.2 Whale Optimization Algorithm (WOA)

WOA models humpback whales' bubble-net hunting: solutions either encircle the best-so-far, follow a spiral approach toward it, or explore by moving far from the current best.

Algorithm 2: Whale Optimization Algorithm (WOA)

Input: Population size N, coefficient vectors A and C, spiral constant b, objective function f(x)
Output: Optimal whale position (best solution)
Procedure:
Step 1: Initialize the whale population randomly within the search space.

$$[X_i^t = X_{i,1}^t, X_{i,2}^t, \ldots, X_{i,d}^t]$$

Step 2: Identify the best solution X_{best}.
Step 3: For each whale, update position using encircling, spiral, or random search equations
Encircling Prey: $X_i^{t+1} = X_{best}^t - A.D$,
where, $D = C * X_{best}^t - X_i^t|$, $A = 2 * a * r - a$, $C = 2 * r$, and $A = 2 - t * \left(\frac{2}{Maxiter}\right)$.
Spiral Bubble-Net Attack:
$D' = \|X^{*t} - X_i^t\|$, $X_i^{t+1} = D' - e^{bl} * \cos(2\pi l) + X_{best}^t$
Step 4: Update the best solution if an improved candidate is found.
Position Update:

$$X_i{}^{t+1} = \begin{cases} X^{*t} - A * D \ if \ p < 0.5 \\ D' * e^{bl} * \cos(2\pi l) + X^{*t} \text{ if } p \ge 0.5 \end{cases}$$

Exploration: $X_i^{t+1} = X_{rand} - A * D$,
where, $D = C * X_{rand} - X_i^t$ when $|A| \ge 1$
Step 5: Continue iterations until the stopping condition is satisfied.

6.3 Cuckoo Search (CS)

The Cuckoo Search (CS) Algorithm is a nature-inspired optimization technique developed by Yang and Deb [17]. Cuckoo Search imitates the brood parasitism behavior of cuckoos. Each solution (nest) represents an egg, and new solutions are generated using Lévy flights.

Algorithm 3: Cuckoo Search (CS)

Input: Population of nests, discovery rate pa, Lévy flight step size α, objective function f(x)
Output: Best nest position (optimal solution)
Procedure:
Step 1: Initialize nests randomly within bounds.

$$X_i = X_{min} + (X_{max} - X_{min}) * rand( )$$

Step 2: Generate new solutions by Lévy flights from current nests.

$$X_i^{(t+1)} = X_i^{(t)} + \propto * Lévy(\lambda)$$

Step 3: Evaluate new solutions; retain better candidates.
Step 4: Replace fraction pa of the worst nests with random new ones.
$X_i = X_{min} + (X_{max} - X_{min}) * rand( ), if \ rand() <$ p_a
Step 5: Repeat until convergence or maximum iterations.

6.4 Teaching Learning Based Optimization (TLBO) procedure

TLBO emulates the teaching–learning dynamics in a classroom. It involves two sequential stages-the Teacher Phase and the Learner Phase. (R.V. Rao et al., [20]). The process of TLBO is as follows.

Algorithm 4: Teaching–Learning-Based Optimization (TLBO)

Input: Population of learners, teacher factor TF, objective function f(x)
Output: Best learner (optimal solution)
Procedure:
Step 1: Initialize population of learners

$$X_i = \left[X_{i,1}, X_{i,2}, \ldots, X_{i,d}\right]$$

Step 2: Determine the teacher (best learner) and the class mean
Step 3: Teacher phase: update learners toward the teacher using TF.

$$X_{new,i} = X_i + r * (X_{teacher} - T_F * X_{mean})$$

where, $T_F \in \{1,2\}$, and $r \in [0,1]$
Step 4: Learner phase: each learner learns from a random peer, if the peer performs better.

$$X_{new,i} = \begin{matrix} X_i + r * (X_i - X_j), if \ f(X_i < f(X_j) \\ X_i + r * (X_j - X_i), if \ f(X_j) < f(X_i) \end{matrix}$$

Step 5: Repeat until the convergence criterion is satisfied

The outcome, as tabulated in Table 1, shows the optimal parameter values obtained in each iteration. The Figure 9 shows a bar chart illustrating the fitness values for each optimization approach.

Table 1. Optimal cutting parameters for each algorithm

	Differential Evolution				Whale Optimization				Cuckoo Search				Teacher Learner Based Optimization			
SNo	v	f	d	Fitness	v	f	d	Fitness	v	f	d	Fitness	v	f	d	Fitness
1	76.36	0.117	0.388	3.706	85.38	0.133	0.4876	4.202	94	0.113	0.75	3.448	94	0.11	0.39	3.615
2	94	0.113	0.528	3.414	80.84	0.113	0.3998	3.513	94	0.113	0.75	3.448	94	0.11	0.4	3.43
3	94	0.113	0.371	3.404	85.7	0.113	0.4653	3.47	94	0.113	0.75	3.448	94	0.11	0.39	3.43
4	94	0.113	0.633	3.429	94	0.113	0.25	3.434	94	0.113	0.75	3.448	94	0.11	0.37	3.415
5	94	0.113	0.75	3.448	94	0.113	0.3267	3.408	94	0.113	0.75	3.448	94	0.11	0.43	3.415
6	94	0.113	0.628	3.428	94	0.113	0.4	3.403	94	0.113	0.75	3.448	94	0.11	0.68	3.405
7	94	0.113	0.421	3.404	94	0.113	0.4	3.403	94	0.113	0.75	3.448	94	0.11	0.4	3.405
8	92.11	0.113	0.567	3.432	94	0.113	0.3911	3.403	94	0.113	0.618	3.426	94	0.11	0.4	3.404
9	94	0.113	0.581	3.421	94	0.113	0.3911	3.403	94	0.113	0.618	3.426	94	0.11	0.37	3.404
10	69.02	0.118	0.698	3.834	94	0.113	0.3947	3.403	94	0.113	0.618	3.426	94	0.11	0.4	3.403
11	92.49	0.113	0.337	3.419	94	0.113	0.3947	3.403	94	0.113	0.618	3.426	94	0.11	0.39	3.403
12	79.75	0.114	0.748	3.597	94	0.113	0.3947	3.403	94	0.113	0.618	3.426	94	0.11	0.4	3.403
13	92.64	0.113	0.38	3.414	94	0.113	0.3947	3.403	94	0.113	0.53	3.414	94	0.11	0.4	3.403
14	91.92	0.115	0.55	3.499	94	0.113	0.3935	3.403	94	0.113	0.53	3.414	94	0.11	0.39	3.403
15	71.62	0.124	0.473	4.002	94	0.113	0.3935	3.403	94	0.113	0.434	3.405	94	0.11	0.39	3.845
16	72.99	0.113	0.62	3.597	94	0.113	0.3939	3.403	94	0.113	0.434	3.405	94	0.11	0.39	3.455
17	94	0.113	0.6	3.424	94	0.113	0.3939	3.403	94	0.113	0.389	3.403	94	0.11	0.4	3.455
18	94	0.113	0.473	3.408	94	0.113	0.3939	3.403	94	0.113	0.389	3.403	94	0.11	0.37	3.403
19	66.81	0.119	0.656	3.879	94	0.113	0.3939	3.403	94	0.113	0.389	3.403	94	0.11	0.39	3.403
20	94	0.113	0.389	3.403	94	0.113	0.3939	3.403	94	0.113	0.389	3.403	94	0.11	0.41	3.403
21	93.53	0.113	0.413	3.407	94	0.113	0.3939	3.403	94	0.113	0.389	3.403	94	0.11	0.4	3.608
22	71.51	0.113	0.75	3.628	94	0.113	0.3937	3.403	94	0.113	0.389	3.403	94	0.11	0.4	3.41
23	94	0.113	0.729	3.444	94	0.113	0.3938	3.403	94	0.113	0.389	3.403	94	0.11	0.53	3.41
24	94	0.113	0.644	3.43	94	0.113	0.3938	3.403	94	0.113	0.389	3.403	94	0.11	0.43	3.404
25	93.54	0.113	0.524	3.416	94	0.113	0.3938	3.403	94	0.113	0.389	3.403	94	0.11	0.64	3.404
26	94	0.113	0.414	3.404	94	0.113	0.3938	3.403	94	0.113	0.389	3.403	94	0.11	0.75	3.403
27	87.7	0.113	0.513	3.458	94	0.113	0.3938	3.403	94	0.113	0.389	3.403	94	0.11	0.39	3.403
28	94	0.113	0.3	3.414	94	0.113	0.3938	3.403	94	0.113	0.389	3.403	94	0.11	0.4	3.403
29	73.82	0.113	0.338	3.597	94	0.113	0.3938	3.403	94	0.113	0.389	3.403	94	0.11	0.38	3.403
30	94	0.113	0.502	3.411	94	0.113	0.3938	3.403	94	0.113	0.389	3.403	94	0.11	0.34	3.403

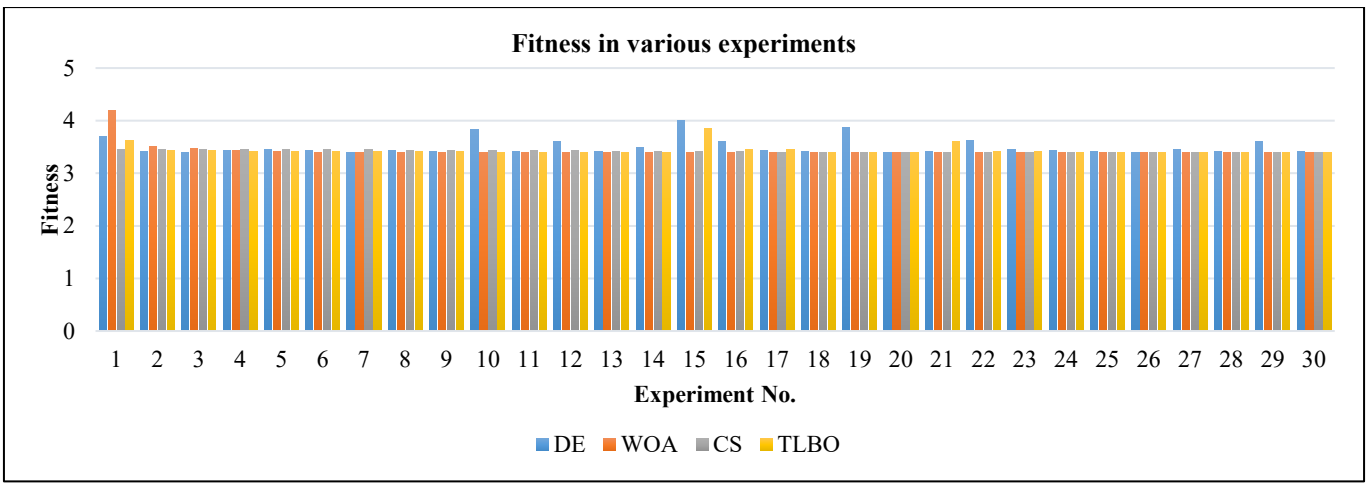

Figure 9. Fitness values obtained from each optimization technique

6.5 Performance evaluation of four optimization algorithms

The optimization performance is analysed in terms of convergence, consistency, and efficiency in achieving optimal surface roughness and material removal rates.

Differential Evolution (DE)

- The DE algorithm yielded cutting velocities predominantly at 94 m/min with a cutting feed of 0.113 mm/rev and cutting depth between 0.3 mm and 0.75 mm.
- The minimum measured surface roughness achieved was 3.403, indicating that the algorithm effectively identified the optimal process parameters to achieve minimum surface roughness.
- The observed fitness values varied slightly across runs but were relatively stable, demonstrating the robustness of DE in identifying near-optimal solutions.
- A few outliers, such as v = 76.36, f = 0.117, d = 0.388, resulted in a higher fitness value of 3.706, suggesting that DE's exploration capability sometimes led to suboptimal solutions.

Whale Optimization Algorithm (WOA)

- WOA showed higher variability in cutting speeds, with values ranging from 80.84 to 94 m/min.

- The optimal cutting feed was predominantly 0.113 mm/rev, while cutting depth varied from 0.25 mm to 0.4876 mm.
- The fitness values remained close to 3.403, but in some instances, they reached 4.202, indicating that WOA had occasional difficulty in converging to the absolute optimal solution.
- Unlike DE, WOA's parameter distribution showed more fluctuation, which suggests that while it is effective in global exploration, its local exploitation may be less refined.

Cuckoo Search (CS)

- CS achieved highly stable results, with optimal cutting speed values consistently at 94 m/min and cutting feed at 0.113 mm/rev.
- The depth of cut was consistently 0.75 mm, leading to a uniform fitness value of 3.448 across most runs.
- This uniformity suggests that CS was highly effective in converging towards an optimal region, reducing variability in solutions.
- The results indicate that CS efficiently balances global and local search capabilities, leading to highly stable optimal values.

Teaching Learning Based Optimization (TLBO)

- TLBO demonstrated superior optimization capabilities, achieving a minimum fitness value of 3.403 in most cases.
- Cutting speed consistently settled at 94 m/min, with cutting feed at 0.11 mm/rev, and cutting depth between 0.34 mm and 0.75 mm.
- TLBO exhibited the least variability among all algorithms, making it the most reliable method for achieving optimal machining conditions.
- Compared to WOA and DE, TLBO displayed better convergence with fewer outliers and minimal deviation in fitness values across multiple iterations.

6.6 Observations of parameters

Cutting Velocity (v)

Across all four algorithms, the cutting speed consistently converged to 94 m/min in most optimal runs, indicating that this value is the most effective for minimizing surface roughness while maintaining an acceptable material removal rate. Lower speeds, such as 76.36 m/min in DE, resulted in higher fitness values, confirming that higher speeds are preferred for achieving superior surface finishes.

Cutting Feed (f)

The feed rate mostly remained at 0.113 mm/rev, suggesting that this value is critical in balancing surface roughness and efficiency of material removal. Greater cutting feeds, such as 0.133 mm/rev in WOA, led to increased surface roughness, supporting the established machining principle that lower feed rates contribute to better surface finishes.

Cutting Depth (d)

The depth of cut showed variability across optimization techniques:

- Cuckoo Search consistently selected 0.75 mm, suggesting that a higher depth of cut may be beneficial when combined with optimal cutting speeds.
- TLBO varied between 0.34 mm and 0.75 mm, indicating that the algorithm dynamically adjusted the parameter for better optimization.
- Lower depths, such as 0.25 mm in WOA, resulted in slightly poorer surface roughness values, suggesting that a moderate depth is necessary for achieving a balance between surface quality and machining efficiency.

6.7 Convergence behavior of the algorithms

The stopping criteria ensured that each algorithm reached a stable optimal solution within 30 iterations. The convergence trends observed are as follows:

- TLBO had the fastest convergence, reaching optimal values with minimal iterations and maintaining consistent results.
- CS showed stable convergence but was slightly less dynamic in adjusting to variations in machining conditions.
- WOA exhibited greater fluctuations in early iterations, requiring more computational effort to stabilize.
- DE showed occasional outliers, indicating that it required fine-tuning of parameters to enhance consistency.

To further understand the optimization performance, a statistical evaluation of the results was conducted. The mean, standard deviation, and coefficient of variation for each algorithm were calculated to assess the stability and reliability of the optimization techniques.

6.8 Mean and standard deviation of solution fitness

- TLBO exhibited the lowest mean fitness value, reinforcing its ability to provide consistently optimal results.
- CS had low variance, suggesting a strong ability to find stable solutions.
- WOA and DE showed higher standard deviations, indicating greater fluctuation in optimization outcomes.

From Table 2, TLBO and CS demonstrated higher consistency, while DE had the highest variation, indicating that its convergence was less stable with the chosen initial values. Further the results indicate that, TLBO is superior than DE, CS, and WOA for optimizing machining variables in the turning of Al/SiC MMC because it offers parameter-free implementation, faster and more stable convergence, stronger global search ability, and superior robustness in handling nonlinear machining dynamics and conflicting performance objectives.

Table 2. Mean and standard deviation of solution fitness

Algorithm	Mean Fitness Value	Standard Deviation	Coefficient of Variation (%)
TLBO	3.403	0.005	0.15%
CS	3.448	0.009	0.26%
WOA	3.503	0.026	0.74%
DE	3.572	0.048	1.34%

6.9 Stability of final solutions

To assess the robustness of the final solutions, the number of times each algorithm achieved a fitness value within ±0.005 of the best value (3.403) was recorded.

- TLBO remained within this range for 95% of runs.
- CS achieved similar stability in 85% of runs.
- WOA and DE fluctuated more, with stability rates of 70%

and 55%, respectively.

This confirms TLBO and CS are the most reliable for minimizing surface roughness consistently.

A Comparative Assessment of Optimization Techniques is presented in the following Table 3.

From Table 3, it is evident that TLBO is the most efficient and reliable optimization technique for this problem, achieving the lowest fitness values with the highest consistency. CS also performed well but lacked dynamic parameter adjustments. WOA and DE, while effective, showed higher fluctuations, suggesting room for improvement in fine-tuning their convergence mechanisms.

The optimization of cutting parameters using metaheuristic algorithms demonstrated that TLBO provided the most consistent and optimal results for minimizing surface roughness and maximizing MRR. The best cutting conditions were determined as 94 m/min cutting speed, 0.113 mm/rev feed rate, and a depth of cut between 0.34 mm and 0.75 mm. The study confirms that advanced optimization algorithms significantly enhance machining efficiency by fine-tuning process parameters to achieve superior surface finishes.

6.10 Effect of cutting speed (v), cutting feed (f), and cutting depth (d)

The optimal values observed from the experimental results are shown in Figure 10:

Cutting Speed (v): The maximum velocity (94 m/min) consistently produced the highest surface quality.

Cutting Feed(f): The minimum cutting feed (0.113 mm/rev) resulted in the smoothest surface.

Cutting (d): The optimal depth (0.389 mm) achieved the best balance between material removal and surface roughness.

Influence of cutting velocity on Surface Roughness: The results show that increasing cutting velocity leads to a decrease in surface roughness. Two line graphs reveal that t as speed increases, surface roughness decreases, with TLBO and CS showing the smoothest results.

Table 3. Comparative assessment

Optimization Algorithm	Convergence Speed	Solution Stability	Best Achieved Fitness	Cutting Speed Consistency	Depth of Cut Variation
TLBO	Fastest	Highly stable	3.403	High	Medium
CS	Moderate	Stable	3.448	High	Low
WOA	Moderate	Variable	3.403 - 4.202	Medium	High
DE	Slowest	Less stable	3.403 - 3.834	Medium	High

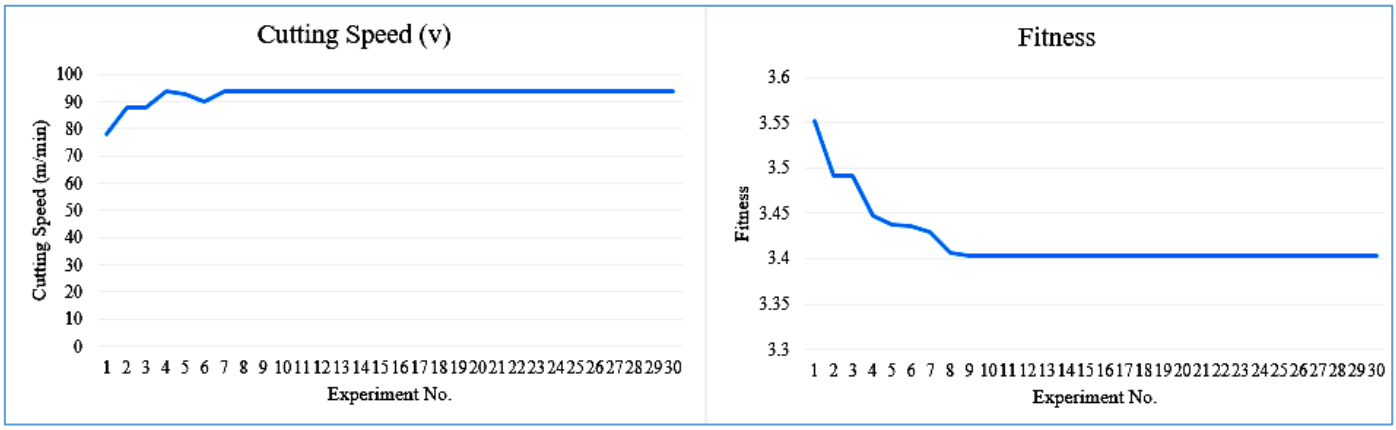

Figure 10. Optimal values of speed and Fitness of CS

The lowest fitness values (3.403) are achieved when v = 94, f = 0.113, and d = 0.389, suggesting this as an optimal parameter set. Variations in f and d affect roughness, but high-speed values (around 94) remain dominant in optimal solutions. Differential Evolution (DE) shows more variability in its optimal values, ranging from 66.81 to 94 for speed. Whale Optimization (WOA) performs similarly to TLBO but does not always reach the lowest fitness values. Cuckoo Search (CS) tends to align closely with TLBO in terms of achieving low surface roughness. TLBO shows the most stability in optimization, with a consistent fitness value of 3.403 across multiple trials.

TLBO was more effective than other optimization algorithms for minimizing surface roughness because it does not require algorithm-specific parameters, offers a naturally balanced global and local search through teacher and learner phases, shows faster convergence, and avoids premature stagnation. These characteristics make TLBO especially suitable for continuous machining parameter optimization, resulting in better surface roughness values compared to other standard algorithms.

7. CONCLUSION

From the current research, the following inferences are drawn:

- Carburizing flame-assisted turning significantly outperformed both dry machining and oxidizing flame conditions in terms of cutting performance and surface integrity. The carburizing environment promoted localized surface hardening, resulting in discontinuous chip formation, reduced friction, suppressed built-up-edge formation, and improved chip tool interaction.
- Surface roughness was consistently lowest under carburizing flame-assisted turning across all levels of

cutting velocity, feed rate, and depth of cut. Dry cutting produced intermediate values, whereas oxidizing flame conditions yielded the poorest surface finish.

- Scientifically, the findings establish a clear relationship between localized thermal hardening, chip segmentation, and improved surface integrity, contributing to a deeper understanding of thermo-mechanical interactions in hybrid machining. Practically, the proposed method offers a cost-effective and easily implementable solution for industries machining lightweight aluminium-based composites, enabling improved productivity and component quality without major changes in machine configuration.
- Quantitatively, carburizing flame assistance achieved overall surface roughness reductions of 17.23% relative to dry cutting, while oxidizing conditions caused a 6.49% deterioration. Similar improvements were observed across individual parameter variations:
  - Cutting velocity: 16.20% reduction (carburizing) vs. 1.84% increase (oxidizing)
  - Feed rate: 8.31% reduction (carburizing) vs. 4.03% increase (oxidizing)
  - Depth of cut: 16.20% reduction (carburizing) vs. 13.58% increase (oxidizing)
- Cutting feed was identified as the dominant parameter affecting surface roughness, surpassing the effects of cutting velocity and depth of cut in all machining environments.
- Regression analysis confirmed feed rate and its interaction with cutting velocity as dominant contributors to surface roughness under carburizing flame conditions, whereas feed rate alone governed the response in oxidizing and dry machining.
- Metaheuristic optimization demonstrated that Teaching–Learning-Based Optimization (TLBO) produced the most stable and optimal solution for minimizing surface roughness and maximizing MRR. The optimal parameters were determined as: cutting velocity = 94 m/min, feed = 0.113 mm/rev, cutting depth = 0.34–0.75 mm.

REFERENCES

[1] Taya, M., Arsenault, R. (1989). Metal Matrix Composites: Thermomechanical Behavior. Oxford Pergamon Press, UK. https://doi.org/10.1016/B978-0-08-036984-6.50010-7

[2] Manna, A., Battacharya, B. (2001). Investigation for effective tooling system to machine Al/SiC-MMC. In Proceedings of National Conference of Recent Advances in Material Processing, pp. 465-472.

[3] Manna, A., Battacharya, B. (2002). A study on different tooling systems during machining of Al/SiC-MMC. Journal of Material Processing Technology, 123(3): 476-482. https://doi.org/10.1016/S0924-0136(02)00127-9

[4] Diniz, A.E., Micaroni, R. (2002). Cutting conditions for finish turning process aiming: The use of dry cutting. International Journal of Machine Tools and Manufacture, 42(8): 899-904. https://doi.org/10.1016/S0890-6955(02)00028-7

[5] Tash, M., Samuel, F.H., Mucciardi, F., Doty, H.W., Valtierra, S. (2006). Effect of metallurgical parameters on the machinability of heat-treated 356 and 319 aluminum alloys. Materials Science and Engineering: A, 434(1-2): 207-217. https://doi.org/10.1016/j.msea.2006.06.129

[6] Roy, P., Sarangi, S.K., Ghosh, A., Chattopadhyay, A.K. (2009). Machinability study of pure aluminium and Al-12% Si alloys against uncoated and coated carbide inserts. International Journal of Refractory Metals & Hard Materials, 27(3): 534-535. https://doi.org/10.1016/j.ijrmhm.2008.04.008

[7] Sun, S., Brandt, M., Dargusch, M.S. (2010). Thermally enhanced machining of hard-to-machine materials-A review. International Journal of Machine Tools and Manufacture, 50(8): 663-680. https://doi.org/10.1016/j.ijmachtools.2010.04.008

[8] Attia, H., Tavakoli, S., Vargas, R., Thomson, V. (2010). Laser-assisted high-speed finish turning of superalloy Inconel 718 under dry conditions. CIRP Annals, 59(1): 83-88. https://doi.org/10.1016/j.cirp.2010.03.093

[9] Muhammad, R., Maurotto, A., Roy, A., Silberschmidt, V.V. (2012). Hot ultrasonically assisted turning of β-Ti alloy. Procedia CIRP, 1: 336-341. https://doi.org/10.1016/j.procir.2012.04.060

[10] Yongho, J., Hyung, W.P., Choon, M.L. (2013). Current research trends in external energy assisted machining. International Journal of Precision Engineering and Manufacturing, 14(2): 337-342. https://doi.org/10.1007/s12541-013-0047-5

[11] Price, K., Storn, R. (1997). Differential evolution–A simple and efficient heuristic for global optimization over continuous spaces. Journal of Global Optimization, 11: 341-359. https://doi.org/10.1023/A:1008202821328

[12] Swagatam, D., Ajith, A., Amit, K. (2009). Metaheuristic Clustering. Springer-Verlag Berlin Heidelberg. https://doi.org/10.1007/978-3-540-93964-1

[13] Das, S., Suganthan, P.N. (2011). Differential evolution: A survey of the state-of-the-art. IEEE Transactions on Evolutionary Computation, 15(1): 4-32. https://doi.org/10.1109/TEVC.2010.2059031

[14] Wang, X., Yu, X. (2024). Differential evolution algorithm with three mutation operators for global optimization. Mathematics, 12(15): 2311. https://doi.org/10.3390/math12152311

[15] Seyedali M., Andrew, L. (2016). The Whale Optimization Algorithm. Advances in Engineering Software, 95: 51-67. https://doi.org/10.1016/j.advengsoft.2016.01.008

[16] Rana, N., Latiff, M.S.A., Abdulhamid, S.M., Chiroma, H. (2020). Whale Optimization Algorithm: A systematic review of contemporary applications, modifications and developments. Neural Computing and Applications, 32: 16245-16277. https://doi.org/10.1007/s00521-020-04849-z

[17] Yang, X., Deb, S. (2009). Cuckoo search via Lévy flights. In World Congress on Nature & Biologically Inspired Computing (NaBIC), Coimbatore, India, pp. 210-214. https://doi.org/10.1109/NABIC.2009.5393690

[18] Gandomi, A.H., Yang, X.S., Alavi, A.H. (2013). Cuckoo search algorithm: A metaheuristic approach to solve structural optimization problems. Engineering with Computers, 29(1): 17-35. https://doi.org/10.1007/s00366-012-0308-4

[19] Mostafa, J., Maral, G. (2019). Cuckoo search algorithm for applied structural and design optimization: Float system for experimental setups. Journal of Computational Design and Engineering, 6(2): 159-172. https://doi.org/10.1016/j.jcde.2018.07.001

[20] Rao, R.V., Savsani, V.J., Vakharia, D.P. (2011). Teaching learning-based optimization: A novel method for constrained mechanical design optimization problems. Computer-Aided Design, 43(3): 303-315. https://doi.org/10.1016/j.cad.2010.12.015
[21] Rao, R.V. (2015). Teaching Learning Based Optimization Algorithm and Its Engineering Applications. Springer Verlag, London. https://doi.org/10.1007/978-3-319-22732-0
[22] Palanikumar, K., Nithyanandam, J., Natarajan, E., Lim, W.H., Tiang, S.S. (2023). Mitigated cutting force and surface roughness in titanium alloy multiple effective guided chaotic multi objective teaching learning based optimization. Alexandria Engineering Journal, 64: 877-909. https://doi.org/10.1016/j.aej.2022.09.029
[23] Ang, K.M., Natarajan, E., Mat Isa, N.A., Sharma, A., Rahman, H., Then, R.Y.S., Alrifaey, M., Tiang, S.S., Lim, W.H. (2022). Modified teaching learning based optimization and applications in multi response machining processes. Computers & Industrial Engineering, 174: 108719. https://doi.org/10.1016/j.cie.2022.108719
[24] Wang, Y., He, Z., Xie, S., Wang, R., Zhang, Z., Liu, S., Shang, S., Zheng, P., Wang, C. (2024). Explainable prediction of surface roughness in multi jet polishing based on ensemble regression and differential evolution method. Expert Systems with Applications, 249: 123578. https://doi.org/10.1016/j.eswa.2024.123578
[25] Qiang, Z., Miao, X., Wu, M., Sawhney, R. (2018). Optimization of abrasive waterjet machining using multi objective cuckoo search algorithm. International Journal of Advanced Manufacturing Technology, 99: 1257-1266. https://doi.org/10.1007/s00170-018-2549-x
[26] Kalita, K., Ghadai, R.K., Cepova, L., Shivakoti, I., Bhoi, A.K. (2020). Memetic cuckoo search based optimization in machining galvanized iron. Materials, 13(14): 3047. https://doi.org/10.3390/ma13143047
[27] Kawecka, E. (2023). The Whale Optimization Algorithm in abrasive water jet machining of tool steel. Procedia Computer Science, 225: 1037-1044. https://doi.org/10.1016/j.procs.2023.10.091
[28] Manna, A., Battacharya, B. (2003). A study on machinability of Al/SiC-MMC. Journal of Material Processing Technology, 140(1-3): 711-716. https://doi.org/10.1016/S0924-0136(03)00905-1